

A performance comparison of series power flow control structures in a smart microgrid

Qusay Salem¹, Khaled Alzaareer², Salman Harasis³

¹Department of Electrical Engineering, King Abdullah II School of Engineering Electrical Engineering, Princess Sumaya University for Technology, Amman, Jordan

²Faculty of Engineering, Philadelphia University, Amman, Jordan

³Department of Electrical Engineering, College of Engineering, Tafila Technical University, Tafila, Jordan

Article Info

Article history:

Received Sep 18, 2021

Revised Mar 2, 2022

Accepted Apr 20, 2022

Keywords:

Injected quadrature voltage control strategy

Line current control strategy

Low-voltage smart microgrid

Reactive power control strategy

Series power flow controller

ABSTRACT

This paper investigates the performance of various power control structures on a series power flow controller comprised as transformerless H-bridge inverter under different operating conditions. This power flow controller connects the main grid with the microgrid as it is seriesly attached with the distribution line. Three different control strategies are implemented to regulate the power flow at the interface point using the series power flow controller. The feasibility of the regulation approaches is verified by varying the modulation index and the reference DC-link voltage during different operation modes. Also, the performance of the control strategies is verified under load divergence condition during two different operation modes. The results showed the efficacy of the developed regulation methods in injecting series voltage at point of common coupling (PCC) either during the capacitive or the inductive operation mode. Also, the obtained results reveal the stability and reliability of the regulation methods and the microgrid operation when either the reference DC-link voltage or the modulation index are increased.

This is an open access article under the [CC BY-SA](https://creativecommons.org/licenses/by-sa/4.0/) license.



Corresponding Author:

Qusay Salem

Department of Electrical Engineering, King Abdullah II School of Engineering Electrical Engineering

Princess Sumaya University for Technology

Khalil Al-Saket St., Amman, Jordan

Email: q.salem@psut.edu.jo

1. INTRODUCTION

An alternative power sources to the traditional ones can be accommodated into the distribution network by the integration of renewable energy sources (RES) using power converters-based power electronic interfaces. However, the increasing perception of RES into the distribution network leads to some concerns regarding the stability and reliability of the entire power system [1]–[4]. Dividing the distribution network into zones in which each zone is termed as a microgrid is the best way to minimize the pressure on the utility grid to control these distributed resources. These microgrids have their own regions and control units and they can operate without the help of the utility grid [5]–[9]. However, to optimize the flow of real power (forward and reverse) between both the main supply and the microgrid without reliance on communication systems which might have full shutdown in case of network failure, installing an in-between device or controller between both networks is necessary, and would facilitate the microgrid operation. Several power flow controller-based power-electronic arrangements have been engaged to satisfy this target. Most used are the back-to-back converter [10], the static synchronous series compensator (SSSC) [11] the distributed static synchronous series compensator (DSSSC) established by cascaded H-bridge inverter [12],

the single phase transformerless H-bridge inverters [13], and the smart transformer [14]. However, the cost, size and complexity, operationality of the control strategy and its appropriacy on the intended controller are the main challenges encountered in power flow control studies. Different control strategies have been applied on these controllers where each control strategy is chosen according to the system requirements, needs, and suitability of its structure on the proposed power flow controller [15], [16].

A methodology to control the active power between the utility and the microgrid using back-to-back converters which eases the flow of real and reactive power between both networks have been proposed in [17]. The proposed system can work in two distinct modes according to the microgrid power requirement. Besides, two new control structures for most favorable series compensation which are indirect and direct control have been proposed to evaluate the robustness of a SSSC linked to a 230 kV grid during both modes of operation either capacitive or inductive [18]. Several modelling approaches for the SSSC have been also proposed for Newton power flow analysis [19], [20]. Furthermore, two control methods which are the variable and fixed DC bus voltage are introduced to control the DSSSC based cascaded H-bridge inverter which connects two distinct feeders from different substations together [21]. An active power point of common coupling (PCC) control method has been introduced in [14] by installing a smart transformer at the interface point between the main network and the microgrid to control the active power exchange between both networks using voltage-based droop control concept. Two novel control strategies applied on a transformerless H-bridge inverter connecting the main grid and the microgrid have been implemented for power flow control between both of them, where their feasibility is verified during different operation modes [13]. A new control methodology has been evolved to run the H-bridge inverter as a power flow controller between the main network and the microgrid [22]. A control method for the line current has also been applied on the same H-bridge inverter which is developed in [23] to control the real power transfer between a grid connected-microgrid. A new active power control method in the stationary reference frame has been applied on a series voltage source converter (VSC) which represents an H-bridge inverter to regulate the transfer of active power at the interface point [24].

In this work, a series power-flow control (SPFC) comprised of transformerless H-bridge inverter is introduced as decentralized controller between the smart microgrid and the main grid. Three distinct control strategies among the existing ones are enforced on the series power flow controller to perform the power flow. A performance comparison between the applied control strategies have been presented. The dynamic behavior of the developed series power flow controller is achieved under three different regulation methods. The developed regulation methods are divided as: i) reactive power control method, ii) line current control method, and iii) injected quadrature voltage control method. The voltage of the series power flow controller is proportional to the line current in the first two control strategies. However, it is independent of the line current in third control strategy. All the regulation methods are verified in different operation modes (capacitive and inductive). A discrimination criterion between the control strategies have also been investigated. This work uses Simulink piecewise linear electrical circuit simulation (PLECS) toolbox to model the power network. The SimPowerSystems toolbox is also equipped to perform the regulation methods of series power flow controller.

2. CONTROL STRATEGIES OF THE SPFC

A transformerless H-bridge inverter running as a series controller for real power is connected between the microgrid and the main grid. A voltage with changeable magnitude and phase angle with reference to the current in the line is introduced by this inverter for controlling the PCC power flow. The inverter determines its operation depending on the power flow direction. If the voltage injected in series is lagging with reference to the line current, it performs as a series capacitive impedance. However, it performs as a series inductive impedance when the voltage is leading. Varying the output voltage of this inverter results in controlling the active and reactive power flow through the line. Thus, the bidirectional real power flow between both networks can be regulated. Power flow control is considered as the primary function of the proposed series power flow controller. Besides, investigation of the power flow with the series power flow controller has been fulfilled by applying the direct and indirect control of the line current. The direct control includes the control of the reactive power and line current, whereas the indirect control comprises the injected quadrature voltage control. A fixed DC-link voltage reference has been adjusted for all control methods. This DC-link voltage reference has been chosen so that the microgrid voltage level is within acceptable limits and the power flow control is reasonable.

2.1. Reactive power control method

The power flow at PCC is regulated by controlling either the active or reactive power as the proposed series power-flow controller didn't include a DC source to preserve the DC-link voltage. The control strategy which is based on reactive power injection from the series power flow controller is presented

in Figure 1. In this control strategy, the in-phase voltage $u_{d,max}$ is extracted by comparing the reference of the DC-link voltage $V_{dc,ref}$ with the capacitor measured voltage V_{dc} and then inserting this difference into a proportional integral (PI) controller. A saturation block is provided to keep the resultant in-phase voltage within the acceptable limits $\pm u_{d,max}$.

The quadrature voltage $u_{q,max}$ which represents the modulation index of this voltage is extracted by comparing the reactive power reference value with the measured reactive power of the series power flow controller and then inserting this difference into another PI controller. Also, in this loop, a saturation block is used to maintain the modulation index in a proper range so that the generated voltage varies in its linear region. The series power flow controller performs an inductive mode of operation if the PI controller output is negative. In this case, a phase shift of $+90^\circ$ with the line current is established. However, the series power flow controller performs a capacitive mode of operation if the PI controller output is positive and consequently a phase shift of -90° with the line current is established. Finally, the phase of the line (or PCC) current is extracted by a phase locked loop (PLL) engagement.

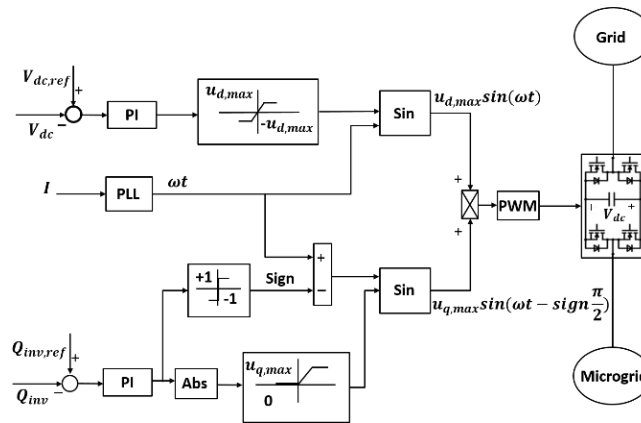


Figure 1. Structure of the reactive power control strategy [25]

2.2. Line current control method

The line current regulation method is presented in Figure 2. The concept of this regulation method is similar to the one presented for reactive power regulation method since the line current is expressed as a function of the reactive voltage injected into the line. However, the reference value of investigating the power flow is a reference current determined by network operators instead of introducing reactive power reference into the system. Indeed, the reference current magnitude (I_{ref}) supported by system operator can control the series power-flow controller operation. This means that the magnitude of line current will not follow the reference value of the current [23]. The reference current is responsible only of injecting series voltage into system grid.

The control of the series power flow controller can be synchronized with system line current with the aid of PLL. Moreover, the voltage injection in the line is ($\pm 90^\circ$) phase-shifted. The line current magnitude is compared with the reference current determined by system operators and using an integral (I) controller, the reference quadrature voltage is produced. Besides, by dividing the measured DC-link voltage over the reference quadrature voltage, the modulation index of quadrature voltage injection ($u_{q,max}$) can be determined. The controller is represented as an integrator so that the output value will never overpass the reference value and the controller will behave smoothly as oscillations is eliminated. The DC-link voltage control and the limiters of $u_{d,max}$, $u_{q,max}$ are the same as in the reactive power control method.

2.3. Injected quadrature voltage control strategy

This control strategy has no link to the line current and is regulated by varying the modulation index resulted from the pulse width modulation technique. The series power flow controller employs the pulse width modulation (PWM) technique to generate a sinusoidal wave from the DC-link capacitor voltage. This control strategy is realized as depicted in Figure 3. A phase locked loop is used to synchronize with the line current positive sequence component. ωt is the PLL output, which is employed to make the necessary transformation of the AC voltages into direct and quadrature components.

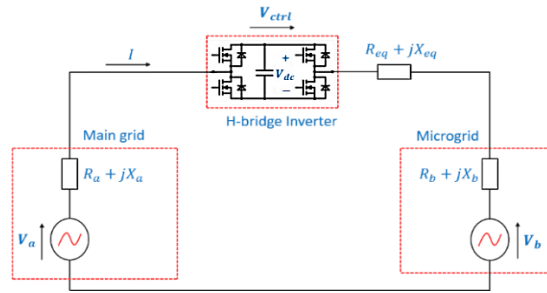


Figure 4. Study system diagram

3.1. Results of the reactive power control strategy

A variation in the reactive power reference from $(-1000$ volt-ampere reactive (VAR) to $+1000$ VAR) at $t=1$ s as shown in Figure 5(a) is performed. Before ($t < 1$ s), the series power flow controller behaves as a capacitive impedance, whereas after ($t > 1$ s), it behaves like an inductive impedance. The controller tracks the step change successfully without any transients. Figure 5(b) demonstrates the series voltage injection which appears at the controller's terminals during both modes of operation. Figures 5(c) and 5(d) show the angle and magnitude for the voltage phase of the series power flow controller in both modes of operation. As seen from the subfigures, the magnitude of voltage injection of the series power flow controller is varied between its capacitive and inductive operation modes. Also, the angle was -90° with reference to the line current in the capacitive mode and $+90^\circ$ in the inductive mode. Figure 5(e) shows the modulation index variation of the series injected voltage during the capacitive and inductive mode, respectively. Furthermore, the DC-link voltage is controlled to its reference value (100 V) as demonstrated in Figure 5(f). The root mean square (RMS) voltage of the grid and microgrid during both operation modes is represented in Figure 5(g). It is noticed how the injected voltage of the series converter affects the microgrid voltage, where it is decreased and increased during different modes of operation, respectively. In Figure 5(h), the microgrid real power is decreased in the inductive mode at ($t > 1$ s) because of the series inductive voltage which increases the voltage of the microgrid. Besides, since the real power control of the microgrid voltage source is dependent on P-V droop control then the active power is changed based on the droop characteristic applied on its reference real power loop generation. Consequently, the grid real power is also decreased. The real power of the series power flow controller (P-inv) has a zero value during both modes of operation since its angle with reference to the line current is $(\pm 90^\circ)$ as represented in Figure 5(d). Figure 5(i) shows the line current in both inductive and capacitive modes of operation. The line current is also reduced when transferring from capacitive to inductive mode due to the reduction of active power transfer from the microgrid to the utility network after switching to inductive mode of operation.

3.2. Results of the line current control strategy

Figure 6(a) shows the step change in the reference line current which changes the measured line current magnitude. When the reference line current is lower than the measured line current, the series power flow controller operates in capacitive mode. However, when the grid operator increases the reference current to be greater than the measured line current magnitude, then the series power flow controller operates in inductive mode. In both cases, a series capacitive or inductive voltage is generated depending on the sign of the difference between the reference current and measured line current. At $t > 1$ s, the line current magnitude is decreased because of injecting series inductive voltage. Figure 6(b) depicts the power of the series power flow controller. The null value of real power during both modes of operation is because the angle is $(\pm 90^\circ)$ with reference to the line current. The reactive power produced from the series converter is a consequence of capacitive and inductive voltage injection, respectively. The DC-link voltage is controlled to its reference value as presented in Figure 6(c). In Figures 6(d)-(f), the injected series voltage of the series power flow controller is appeared as 100 V peak to peak and the magnitude of the same voltage is around 60 V during both operation modes. The angle of the voltage is appeared as $\pm 90^\circ$ with reference to the line current during both modes of operation, respectively. The RMS voltage of the grid and microgrid voltage sources is demonstrated in Figure 6(g). The RMS voltage of the microgrid is varied because of injecting capacitive and inductive voltage into the line, respectively. This voltage variation in the microgrid side has changed its generated real power as shown in Figure 6(h). In accordance with the P-V droop characteristic, the microgrid real power is reduced as a result of the voltage increase. Also, the real power at the main grid is reduced since the real power export from the microgrid is reduced. Figure 6(i) shows the series injected voltage modulation index during the capacitive and inductive modes, respectively.

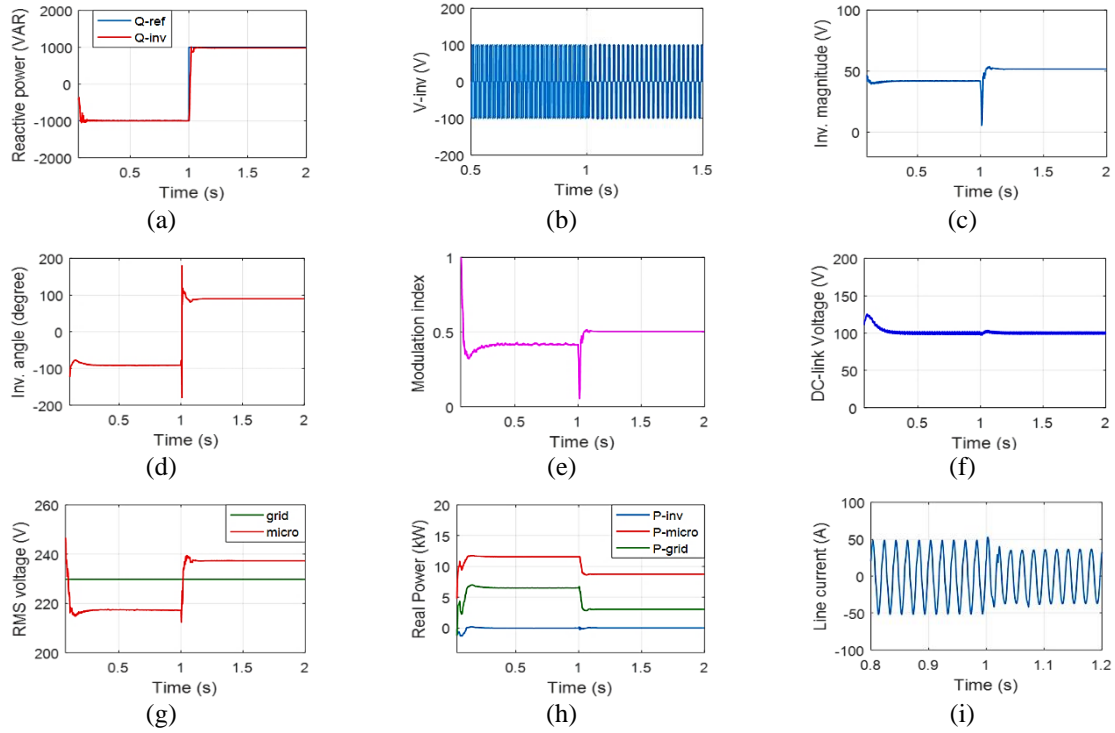


Figure 5. System performance under the reactive power control strategy (a) reference and measured reactive power of the inverter, (b) inverter peak to peak voltage, (c) inverter voltage magnitude, (d) inverter phase angle, (e) modulation index, (f) inverter DC-link voltage, (g) RMS voltage of the grid and the microgrid, (h) real power of the inverter, microgrid, and the grid, and (i) line current

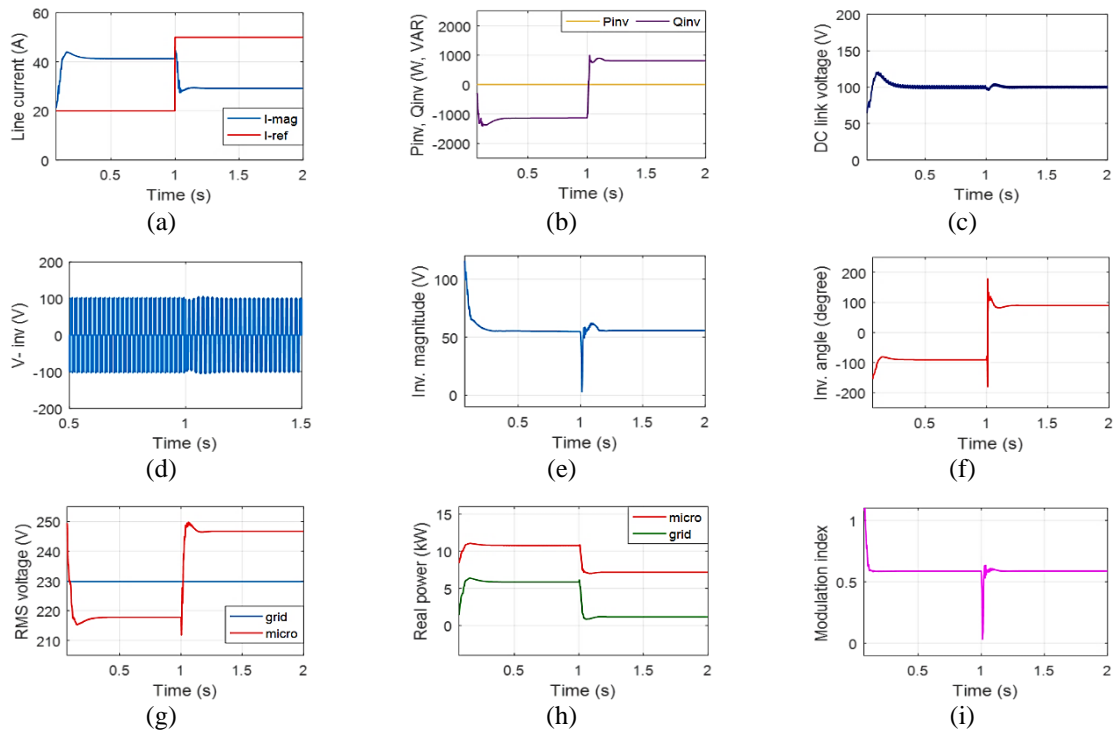


Figure 6. System performance under the line current control strategy (a) reference and measured line current, (b) real and reactive power of the inverter, (c) inverter DC-link voltage, (d) inverter peak to peak voltage, (e) inverter voltage magnitude, (f) inverter phase angle, (g) RMS voltage of the grid and the microgrid, (h) real power of the microgrid and the grid, and (i) modulation index

3.3. Results of the quadrature voltage control method

In this regulation method, the quadrature voltage injected is regulated by using the modulation index as it has no relation to the line current. A variation in the quadrature voltage reference ($V_{q,ref}$) from (+40 V to -40 V) at $t = 1$ s is represented in Figure 7(a). Before ($t < 1$ s), the series power flow controller operates in capacitive mode, whereas after ($t > 1$ s), it operates in inductive mode. The measured injected quadrature voltage tracks the step change reference successfully in both operation modes. Figure 7(b) shows how the voltage of the DC-link is kept constant and regulated to its reference value during both operation modes. In accordance with the quadrature voltage reference, the injected voltage is controlled by altering the modulation index during the capacitive and inductive modes as presented in Figure 7(c). Figure 7(d) shows the voltage which takes shape at the series converter terminals during both operation modes. Figure 7 (e)-(f) depict the series power flow controller magnitude and angle of the voltage phase in both modes of operation with reference to the line current. The magnitude of the injected voltage at the series power flow controller is raised at ($t > 1$ s) as a consequence of the step change in the reference quadrature voltage and consequently the modulation index, in which the series power flow controller switches from capacitive to inductive operation mode. Also, the phase angle was -90° with respect to the line current in the capacitive mode and $+90^\circ$ in the inductive mode. The RMS voltage of the grid and microgrid during both operation modes are within acceptable limits as depicted in Figure 7(g). The injected voltage of the series power flow controller decreases the microgrid RMS voltage in the capacitive mode, whilst it increases the microgrid RMS voltage in the inductive mode. In Figure 7(h), the microgrid real power is increased in the capacitive mode at ($t < 1$ s) as a result of the decreased RMS voltage. However, the microgrid real power is decreased in the inductive mode at ($t > 1$ s) as a result of the increased RMS voltage. The variation in microgrid active power is a result of the droop characteristic between the produced real power and the RMS voltage of the microgrid voltage source. Besides, the grid real power is also reduced due to the reduced real power import from the microgrid. Figure 7(i) shows the real and reactive power of the series power flow controller. The null value of real power during both operation modes is attained since the angle is ($\pm 90^\circ$) phase shifted as depicted in (f). The reactive power generated from the series power flow controller is a result of varying the injected quadrature voltage reference, and consequently the modulation index of the voltage injection.

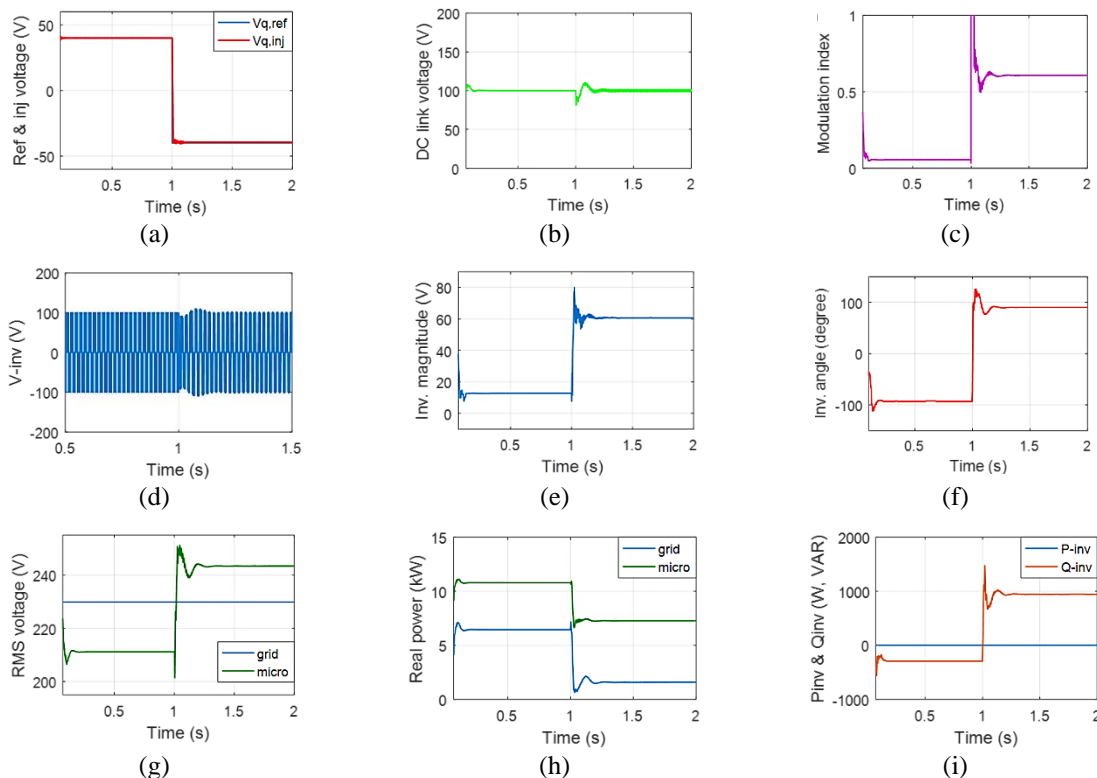


Figure 7. System performance under the injected quadrature voltage control strategy (a) reference and measured injected quadrature voltage, (b) inverter DC-link voltage, (c) modulation index, (d) inverter peak to peak voltage, (e) inverter voltage magnitude, (f) inverter phase angle, (g) RMS voltage of the grid and the microgrid, (h) real power of the microgrid and the grid, and (i) real and reactive power of the inverter

4. DISCRIMINATION CRITERIA BETWEEN THE CONTROL STRATEGIES

When regulating the power-flow in 400 V low-voltage distribution system using the power flow controller, some limitations should be considered. The RMS voltage of the microgrid should maintain an acceptable range according to EN 50160 standard [26] so that the microgrid can still function in its grid-connected mode. Otherwise, the microgrid will be disconnected and worked in island mode. Therefore, the injected voltage modulation index or the DC-link voltage reference should be assigned, in which they will not lead to exceed the specified limits of the microgrid voltage and malfunction of the control strategy as well. Furthermore, the PLL cannot accurately track the phase of current and the control strategies might misoperate if the voltage injected is greater than a determined value.

In accordance with the reactive power control method, the effect of increasing the modulation index ($u_{q,max}$) and the DC-link voltage reference on the microgrid RMS voltage during either capacitive or inductive operation mode is shown in Figures 8(a) and 8(b). As the modulation index is increasing, the RMS voltage is stable and within acceptable limits during the capacitive mode ($t < 1$ s). However, higher oscillations and limits overshoot are noticed during the inductive mode ($t > 1$ s). In another simulation, the modulation index is assigned as fixed value and the reference DC-link voltage is increased to investigate the influence on the microgrid RMS voltage. During the capacitive mode, the RMS voltage is again stable and running within the boundaries. However, the RMS voltage is getting unstable and has also higher oscillations as the reference DC-link voltage is increasing in the inductive mode.

The same procedure is applied with the line current control strategy as demonstrated in Figures 8(c) and 8(d). When $M = 1$, the RMS voltage oscillates beyond acceptable limits and depicts large oscillations during the capacitive mode ($t < 1$ s). In the inductive mode ($t > 1$ s), the RMS voltage has exceeded the boundaries without large oscillations. Furthermore, increasing the reference DC-link voltage causes the RMS voltage to deviate from the normal operation during the inductive and capacitive modes of operation. In the capacitive mode, the RMS voltage is within limits but with unstable voltage oscillation. However, in the inductive mode it exceeds the limits with stable voltage oscillation.

In the control method of injected quadrature voltage, the modulation index is increased by means of increasing the quadrature voltage reference ($V_{q,ref}$) and the increasing ratio of the reference DC-link voltage is chosen as 100 V so that the influence on the RMS voltage is more obvious. As demonstrated in Figures 8(e) and 8(f), the RMS voltage exhibits stable oscillation in both modes of operation as the modulation index is increasing. However, it goes beyond acceptable limits during the inductive operation mode. With increasing the reference DC-link voltage, the RMS voltage stays within limits as the reference DC-link voltage is between ($100\text{ V} < V_{DC,ref} < 200\text{ V}$) during both modes of operation. If $V_{DC,ref} > 200\text{ V}$, then the control strategy is malfunctioned, and the RMS voltage oscillates out of the range with large transients.

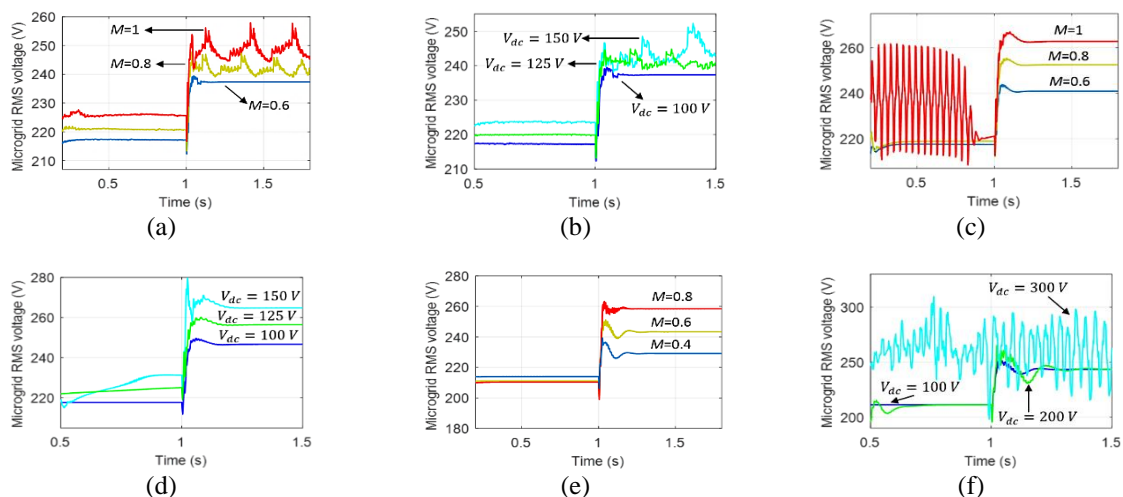


Figure 8. Microgrid RMS voltage with increasing the modulation index and the reference DC-link voltage (a) RMS voltage by increasing the modulation index in the reactive power control method, (b) RMS voltage by increasing the DC-link voltage in the reactive power control method, (c) RMS voltage by increasing the modulation index in the line current control method, (d) RMS voltage by increasing the DC-link voltage in the line current control method, (e) RMS voltage by increasing the modulation index in the quadrature voltage control method, and (f) RMS voltage by increasing the DC-link voltage in the quadrature voltage control method

Figures 9(a) and 9(b) show the comparison between the three control strategies in the capacitive and inductive modes, respectively when a load divergence is occurred between ($1 s < t < 1.5 s$). The three control strategies have shown good performance for regulating the series power flow controller either in the capacitive or inductive mode under the load divergence condition. In the capacitive mode, the transported real power is better promoted by the injected quadrature voltage control strategy than the reactive power and the line current control strategies. However, in the inductive mode, it is notable that the transmitted power is better promoted by the line current control strategy than the reactive power and injected quadrature voltage control strategies.

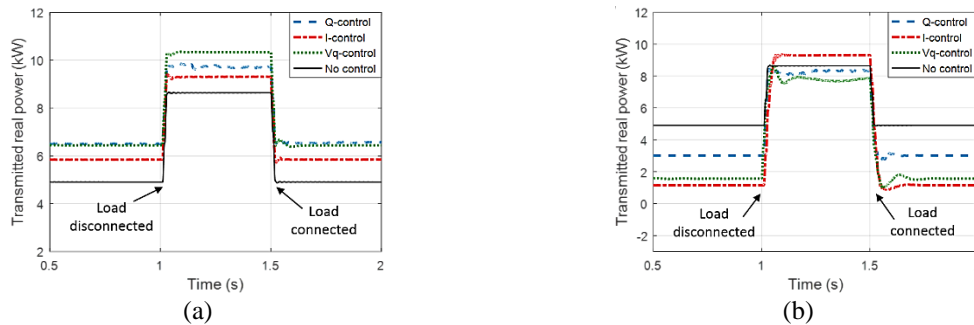


Figure 9. Comparison of the control strategies under load divergence (a) transmitted real power under load divergence during the capacitive operation mode and (b) transmitted real power under load divergence during the inductive operation mode

5. CONCLUSION

In this paper, modeling, and analysis of a smart microgrid connection to the utility network including the series power flow controller is investigated. In accordance with this modeling, three control strategies were developed to control the power flow at PCC and their performance were evaluated during either the capacitive or the inductive mode of operation. It was clear from the attained results that the microgrid RMS voltage was exceeding the limits and the control strategies were malfunctioned when either the modulation index or the reference DC-link voltage is increased. Furthermore, it was observed that the transported real power is better promoted by the injected quadrature voltage control strategy during the capacitive mode. However, the line current regulation method has shown better performance than the other control strategies during the inductive mode.

REFERENCES

- [1] J. M. Guerrero, P. C. Loh, T. Lee, and M. Chandorkar, "Advanced Control Architectures for Intelligent Microgrids—Part II: Power Quality, Energy Storage, and AC/DC Microgrids," in *IEEE Transactions on Industrial Electronics*, vol. 60, no. 4, pp. 1263–1270, April 2013, doi: 10.1109/TIE.2012.2196889.
- [2] M. A. Hossain, H. Pota, M. Hossain, and F. Blaabjerg, "Evolution of Microgrids with Converter-Interfaced Generations: Challenges and Opportunities," *International Journal of Electrical Power & Energy Systems*, vol. 109, pp. 160–186, July 2019, doi: 10.1016/j.ijepes.2019.01.038.
- [3] A. Hirsch, Y. Parag, and J. Guerrero, "Microgrids: A review of technologies, key drivers, and outstanding issues," *Renewable and Sustainable Energy Reviews*, vol. 90, pp. 402–411, July 2018, doi: 10.1016/j.rser.2018.03.040.
- [4] A. Bidram and A. Davoudi, "Hierarchical Structure of Microgrids Control System," in *IEEE Transactions on Smart Grid*, vol. 3, no. 4, pp. 1963–1976, December 2012, doi: 10.1109/TSG.2012.2197425.
- [5] M. Wameryd, M. Hakansson, and K. Karltop, "Unpacking the complexity of community microgrids: A review of institutions' roles for development of microgrids," *Renewable and Sustainable Energy Reviews*, vol. 121, p. 109690, April 2020, doi: 10.1016/j.rser.2019.109690.
- [6] C. Xu and W. Lu, "Development of smart microgrid powered by renewable energy in China: current status and challenges," *Technology Analysis & Strategic Management*, vol. 131, no. 5, pp. 563–578, 2019, doi: 10.1080/09537325.2018.1524864.
- [7] S. D'silva, M. Shadmand, S. Bayhan, and H. Abu-Rub, "Towards Grid of Microgrids: Seamless Transition between Grid-Connected and Islanded Modes of Operation," in *IEEE Open Journal of the Industrial Electronics Society*, vol. 1, pp. 66–81, 2020, doi: 10.1109/OJIES.2020.2988618.
- [8] V. Lavanya and N. S. Kumar, "Control strategies for seamless transfer between the grid-connected and islanded modes of a microgrid system," *International Journal of Electrical and Computer Engineering (IJECE)*, vol. 10, no. 5, pp. 4490–4506, October 2020, doi: 10.11591/ijece.v10i5.pp4490-4506.
- [9] M. Ganjian-Aboukheili, M. Shahabi, Q. Shafiee, and J. M. Guerrero, "Seamless Transition of Microgrids Operation From Grid-Connected to Islanded Mode," in *IEEE Transactions on Smart Grid*, vol. 11, no. 3, pp. 2106–2114, May 2020, doi: 10.1109/TSG.2019.2947651.
- [10] D. Casadei, G. Grandi, C. Rossi, A. Trentin and L. Zari, "Comparison between back-to-back and matrix converters based on thermal stress of the switches," *2004 IEEE International Symposium on Industrial Electronics*, vol. 2, pp. 1081–1086, 2004, doi: 10.1109/ISIE.2004.1571964.
- [11] A. H. Norouzi and A. M. Sharaf, "Two control schemes to enhance the dynamic performance of the STATCOM and SSSC," in *IEEE Transactions on Power Delivery*, vol. 20, no. 1, pp. 435–442, January 2005, doi: 10.1109/TPWRD.2004.839725.
- [12] M. Saradarzadeh, S. Farhangi, J. L. Schanen, P. O. Jeannin, and D. Frey, "Reversing the power flow in the looped electrical distribution network by using a Cascaded H-bridge D-SSSC," *2011 2nd Power Electronics, Drive Systems and Technologies Conference*, 2011, pp. 193–198, doi: 10.1109/PEDSTC.2011.5742415.

- [13] Q. Salem and J. Xie, "Decentralized power control management with series transformerless H-bridge inverter in low-voltage smart microgrid based P/V droop control," *International Journal of Electrical Power & Energy Systems*, vol. 99, pp. 500–515, July 2018, doi: 10.1016/j.ijepes.2018.01.047 .
- [14] T. L. Vandoom, J. D. M. De Kooning, B. Meersman, J. M. Guerrero, and L. Vandeveld, "Voltage-based control of a smart transformer in a microgrid," in *IEEE Transactions on Industrial Electronics*, vol. 60, no. 4, pp. 1291–1305, April 2013, doi: 10.1109/TIE.2011.2165463.
- [15] L. Wang and Q. Vo, "Power Flow Control and Stability Improvement of Connecting an Offshore Wind Farm to a One-Machine Infinite-Bus System Using a Static Synchronous Series Compensator," in *IEEE Transactions on Sustainable Energy*, vol. 4, no. 2, pp. 358–369, April 2013, doi: 10.1109/TSTE.2012.2225156.
- [16] D. Rai, S. O. Faried, G. Ramakrishna, and A. Edris, "An SSSC-based hybrid series compensation scheme capable of damping subsynchronous resonance," in *IEEE Transactions on Power Delivery*, vol. 27, no. 2, pp. 531–540, April 2012, doi: 10.1109/TPWRD.2011.2175253.
- [17] R. Majumder, A. Ghosh, G. Ledwich, and F. Zare, "Power Management and Power Flow Control with Back-to-Back Converters in a Utility Connected Microgrid," in *IEEE Transactions on Power Systems*, vol. 25, no. 2, pp. 821–834, May 2010, doi: 10.1109/TPWRS.2009.2034666.
- [18] M. El Moursi, A. M. Sharaf, and K. El-Arroudi, "Optimal control schemes for SSSC for dynamic series compensation," *Electric Power Systems Research*, vol. 78, no. 4, pp. 646–656, April 2008, doi: 10.1016/j.epr.2007.05.009.
- [19] Y. Zhang and Y. Zhang, "A novel power injection model of embedded SSSC with multi-control," *Electric Power Systems Research*, vol. 76, no. 5, pp. 374–381, March 2006, doi: 10.1016/j.epr.2005.06.008.
- [20] S. Kamel, F. Jurado, and Z. Chen, "Power flow control for transmission networks with implicit modeling of static synchronous series compensator," *International Journal of Electrical Power and Energy Systems*, vol. 64, pp. 911–920, 2015, doi: 10.1016/j.ijepes.2014.08.013.
- [21] M. Saradarzadeh, S. Farhangi, J. L. Schanen, P. O. Jeannin, and D. Frey, "Application of cascaded H-bridge distribution-static synchronous series compensator in electrical distribution system power flow control," *IET Power Electronics*, vol. 5, no. 9, pp. 1660–1675, November 2012, doi: 10.1049/iet-pe.2012.0087.
- [22] Q. Salem, L. Liu, and J. Xie, "Dual Operation Mode of a Transformerless H-Bridge Inverter in Low-Voltage Microgrid," in *IEEE Transactions on Industry Applications*, vol. 55, no. 5, pp. 5289–5299, Sept.-Oct. 2019, doi: 10.1109/TIA.2019.2917807.
- [23] Q. Salem and J. Xie, "A Novel Line Current Control Strategy to Control the Real Power Flow at PCC Using H-bridge Inverter," *International Journal of Power Electronics and Drive System (IJPEDS)*, vol. 9, no. 2, pp. 602–609, June 2018, doi: 10.11591/ijped.v9.i2.pp602-609.
- [24] Q. Salem and J. Xie, "Active power control using an alternative series connection scheme between the utility grid and Microgrid," *2016 IEEE 16th International Conference on Environment and Electrical Engineering (EEEIC)*, 2016, pp. 1–5, doi: 10.1109/EEEIC.2016.7555439.
- [25] Q. Salem, *A transformerless H-bridge inverter as a bidirectional power flow controller in a microgrid based P/V droop control*, Doctoral dissertation, Universität Ulm, 2020, doi: 10.18725/OPARU-29526.
- [26] "IEEE Standard for Interconnecting Distributed Resources with Electric Power Systems," in *IEEE Std 1547-2003*, pp.1–28, July 2003, doi: 10.1109/IEEESTD.2003.94285.

BIOGRAPHY OF AUTHORS



Qusay Salem    has been awarded the Ph.D degree in Electrical Power and Energy Engineering from University of Ulm–Germany, in 2020. He received the B.Sc. and M.Sc. Degree both in Electrical Power Engineering from University of Mutah and Yarmouk University–Jordan, in 2009 and 2013, respectively. Currently, he serves as an assistant professor with the Department of Electrical Engineering at Princess Sumaya University for Technology. His research interests include power control and energy management in low-voltage smart microgrids. He can be contacted at email: q.salem@psut.edu.jo.



Khaled Alzaareer    received the Ph.D degree in Electrical Engineering/Power Systems from Quebec University (ETS), Montreal, QC, Canada in December 2020. He also received the bachelor's and master's degrees in electrical power engineering from Yarmouk University, Irbid, Jordan, in 2010 and 2012, respectively. His research interests are smart grid, sensitivity analysis, renewable energy integration, voltage stability and control. He can be contacted at email: kalzaareer@philadelphia.edu.jo.



Salman Harasis    received the B.Sc. degree in electrical power engineering from Tafila Technical University, Tafila, Jordan, in 2009. Received the M.Sc. degree in electrical engineering from Polytechnic University of Bucharest, Bucharest, Romania, in 2013. Received the Ph.D. degree in electrical engineering from the University of Akron, OH, USA in 2020. He is currently an assistant professor with the Department of Electric power and Mechatronics engineering, Tafila Technical University. His research interests include control of power systems and microgrids, renewable energy, power electronics, and motor drives for transportation electrification applications. He can be contacted at email: Salmanharasis@ttu.edu.jo.